

Generating meshes for tidal wetland modeling using light detection and ranging (LiDAR) data

Ramona Stammermann and Michael Piasecki

ABSTRACT

A high resolution model mesh was required to numerically simulate sediment transport in tidal marshes. The timing of flooding is dependent on the tidal marsh ground elevation, which requires accurate topographic elevation data. The tidal prism of the marsh is determined by the volume provided by tidal channels in the system. Hence, their location and bathymetry needed to be represented adequately. Due to the high spatial variability and inaccessibility of marshes, remote sensing techniques such as light detection and ranging (LiDAR) are a significant resource for elevation data. LiDAR measures the highest elevation of elements. To determine the bare ground elevation, filter techniques exist but are often inadequate to eliminate elevation errors that are introduced by the vegetation of marshes. We introduce a simple method to remove remaining vertical elevation errors in high resolution digital terrain models (DTMs) of vegetated marshes and present an approach to determine the bathymetry of tidal channels based on a limited number of cross-sectional measurements. Forcing polygons for mesh generation were extracted from the DTMs to assure an accurate spatial representation of the marsh. DTMs ($2 \times 2 \text{ m}/1 \times 1 \text{ m}$) derived from LiDAR data from the Blackbird Creek Reserve and Bombay Hook National Wildlife Refuge in Delaware, USA, were used.

Key words | bathymetry, LiDAR, marshes, mesh generation, numerical modeling

Ramona Stammermann (corresponding author)
Department of Civil, Architectural and
Environmental Engineering (CAEE),
Drexel University,
3141 Chestnut Street,
Philadelphia,
PA 19104,
USA
E-mail: rs487@drexel.edu

Michael Piasecki
Department of Civil Engineering,
City College of New York,
160 Convent Ave.,
New York City,
NY 10031,
USA

INTRODUCTION

The role of marshes as an ecological resource and their importance for their adjacent water body has been increasingly recognized in recent decades (Boorman 1999; Allen 2000; Mendelssohn & Kuhn 2003; Kathilankal *et al.* 2008). For successful management, preservation, and restoration efforts for marshes, numerical models can serve as a useful tool to assess alternative measures and their potential for success or failure. Given an appropriate numerical integration scheme of the governing equations and also the dimensionality (0D/1D/2D/3D) of the analytical approach, the challenge is to generate a numerical model mesh that is sufficiently refined to capture necessary detail, but still offers an adequate model efficiency at run time, i.e. real-time to model CPU-time ratios larger than one. The high degree of dry to temporarily and constantly inundated land ratios in addition to a complex system of meandering and interconnected channels would typically demand a large number

of measurement stations to adequately map out these features. Ground-based surveys in densely vegetated and inaccessible marshes are time-consuming and high spatial resolution can only be accomplished with great resources.

For this purpose, remote sensing technologies such as light detection and ranging (LiDAR) have the potential to provide a data set that can aid in overcoming these difficulties. Typically, LiDAR measures the ground elevation at a spacing of 0.5 to 5 m (Abdullah *et al.* 2012). An additional advantage is that LiDAR data are now available for many areas of the United States, for instance through the NOAA Coastal Services Center (NOAA 2012). The accuracy of vertical elevations in digital terrain models (DTMs) depends on the observed land type and applied filtering methods. In urban or forested areas precisely identifiable references, such as buildings, streets, and trees, allow for easier registration and bias correction of LiDAR data. Much progress

has been made in the development of filtering algorithms for urban flood modeling applications (Abdullah *et al.* 2011, 2012; Bates 2012; Sampson *et al.* 2012). Yet, the relatively short vegetation of wetlands does not provide detectable differences between first and last LiDAR returns, and the density of the vegetation often prevents direct LiDAR ground hits. It is therefore uncertain if LiDAR returns are really backscattered from the ground or from some higher point in the canopy. Recent studies revealed that LiDAR derived DTMs still report significant errors in areas of low and dense vegetation (Athearn *et al.* 2010; Meng *et al.* 2010; Hladik & Alber 2012; Rose *et al.* 2013). Selecting the right filter algorithms out of the many available requires a certain level of expertise and sufficient hardware and software capabilities are needed to process high density data sets (Meng *et al.* 2010). Hence, application of already existing DTMs can be preferable for new users or for projects that cannot afford their own LiDAR survey. Unless filtering methods were used that were specifically developed to derive a DTM of vegetated wetlands, it is very likely that regional DTMs contain a significant vertical error above tidal marshes and respective assessments and adjustments are advisable.

Airborne LiDAR bathymetry systems are capable of measuring water from 1.5 to 60 m depths (Wang & Philpot 2007), but are limited by water clarity (Gilvear *et al.* 2004; Athearn *et al.* 2010). However, water depths less than 1.5 m occur frequently in marshes and turbid water prevents the use of LiDAR in wetlands. While the location of channel systems can be easily extracted from the DTM, water depths have to be measured separately.

To the authors' knowledge this is the first paper that provides a full-suite approach to unstructured mesh generation for wetland hydrodynamic numerical models, including the extraction of forcing polygons, and the determination of topographical and bathymetrical elevations. The use of already available DTMs from public sources and a limited requirement for additional field surveys offers a solution for institutions and users with limited resources. Simple methods to improve bare ground elevations in DTMs of vegetated marshes and to determine the bathymetry of tidal channels from cross-sectional measurements are introduced. The extraction of outlines of tidal channels for mesh triangulation is described, which was applied to a two-dimensional

hydrodynamic and morphodynamic numerical modeling study with the model system Marina2D (Milbradt 2012). Past research has been done on how to interpret LiDAR and other remote sensing data in terms of vegetation classification (Rosso *et al.* 2006; Huang *et al.* 2009; Collin *et al.* 2010), how to find waterlines and tidal channels in flooded vegetation (Horritt *et al.* 2003; Mason *et al.* 2006), and how to separate ground from low vegetation cover (Wang *et al.* 2009). These were used as guidelines, but had to be adjusted for the available type and resolution of data used for this project.

STUDY AREA AND MODEL DOMAIN

The areas of interest were marshes of the Blackbird Creek Reserve and the Bombay Hook National Wildlife Refuge in the state of Delaware located on the western shore of the Delaware Bay on the US East Coast (Figure 1). The Blackbird Creek Reserve is part of the National Estuarine Research Reserves System and ongoing research, monitoring, and field studies in this area is supported by the Delaware Department of Natural Resources and Environmental Control (DNREC 2013). The marshes were selected (i) because they show first signs of degradation and (ii) because of monitoring programs that yielded a reasonably sized *in situ* data set. The Bombay Hook National Wildlife Refuge already exhibits significant losses through coastal inundation. It is estimated that since 1979, it has lost 12% of its wetland area (Valencik 2010).

The outline for the Blackbird Creek marsh model was chosen based on the results of the Sea Level Affecting Marshes Model (SLAMM) (Kearney & Stevenson 1991). Scenarios for 0.5, 1.0 and 1.5 m sea level rise were calculated, resulting in boundaries for maximum flood extension. The outline for the 1.5 m sea level rise scenario (Figure 1, white line inside Blackbird Creek limits) was used as a guideline to determine the model area. The final outline includes a stretch of the Delaware River and a generous buffer zone landward of the marsh area to ensure coverage of all possible flood areas (Figure 1, black line).

The landward extent of the Bombay Hook model was determined using aerial pictures from Google Earth by

manually tracing streets in between Bombay Hook and its adjacent marsh systems (Figure 1, black and white line landward of Bombay Hook). Although the area of interest mainly consists of the stressed marsh area north of Leipsic River, the whole marsh system was modeled as a network of interconnected channel systems. Modeling only the area of interest would result in an additional degree of difficulty for the model forcing, since additional information about channel boundary conditions would be necessary. In comparison, for the whole system only tidal inflow from the Delaware Bay and discharge of the Leipsic River were needed as boundary conditions (Figure 1).

DIGITAL TERRAIN MODELS

LiDAR data for the Blackbird Creek Reserve

In 2007 LiDAR data were acquired for Kent and New Castle Counties for DNREC's Delaware Coastal Programs Section (NOAA 2007). The LiDAR acquisition campaign was designed to provide a high density set of mass points

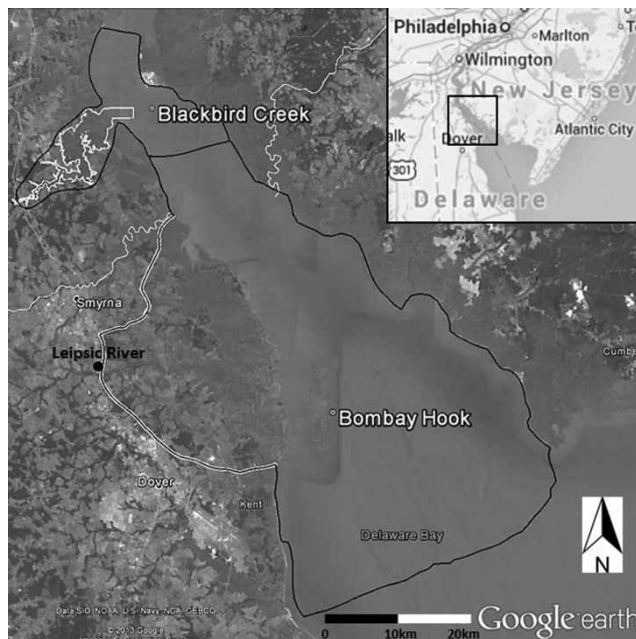


Figure 1 | Study area overview and model domain boundaries.

within the defined areas which made them an ideal source for the development of contours for use in hydraulic/hydrologic model development (it is available for download at the Digital Coast website from NOAA Coastal Services Center; NOAA 2012). Seven missions were flown between 31 March and 5 April 2007 by Sanborn Map Company, Inc. using the Leica Systems ALS50 LiDAR system. The coverage was classified to extract a bare earth DTM (Figure 2) in $2\text{ m} \times 2\text{ m}$ resolution using TerraScan software by Terrasolid Limited of Helsinki, Finland. Detailed information about applied filtering methods was not provided in the metadata. For well-defined points, such as streets and houses, the vertical accuracy was $\pm 18.5\text{ cm}$, and $\pm 37.0\text{ cm}$ for points in heavily vegetated areas, such as the marsh.

LiDAR data for the Bombay Hook National Wildlife Refuge

In 2011 NOAA Coastal Services Center, in partnership with DNREC, commissioned a third party (Dewberry) to develop an accurate surface elevation data set derived

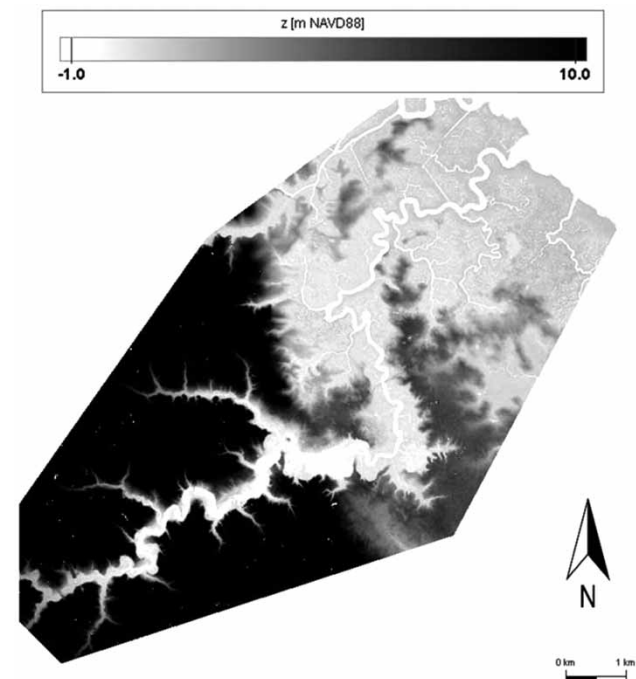


Figure 2 | DTM Blackbird Creek Reserve.

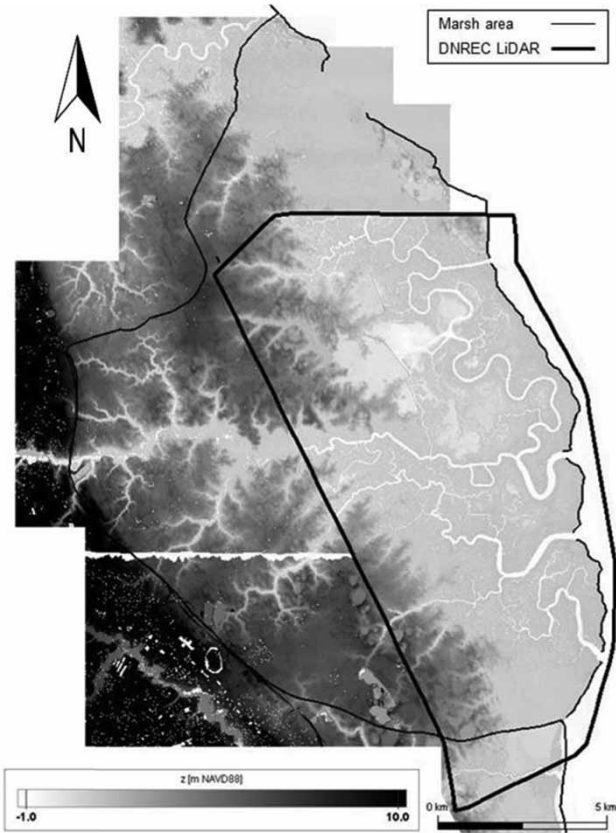


Figure 3 | DTMs Bombay Hook National Wildlife Refuge: DNREC (inside heavy line) and KNC.

from high-accuracy LiDAR for the Bombay Hook National Wildlife Refuge (Figure 3, inside heavy line). The LiDAR aerial acquisition was conducted from 18 April through 20 April 2011. Flights were timed with low water conditions to ensure the highest availability of exposed ground. The vertical accuracy is ± 10 cm for comparisons with checkpoint elevations. The fundamental vertical accuracy tested 14 cm and the consolidated vertical accuracy 11 cm at the 95% confidence level, a significantly higher accuracy than the Kent–New Castle (KNC) data set used for Blackbird Creek. A few areas still appeared noisy in the developed DTMs; these areas are generally vegetated. The full point cloud was analyzed for these areas and the lowest available points were determined and classified as ground for each pixel. The processed and filtered data are available in a $1\text{ m} \times 1\text{ m}$ resolution DTM (Dewberry 2011).

The DNREC LiDAR data set did not fully cover the whole model area, but concentrated on tidal marshes in

the center. For the remaining area the aforementioned KNC DTM was used. Direct comparison of elevations above vegetated areas from the two data sets revealed the importance of filter techniques that are adjusted for vegetated marshes. While distinctly defined elevations such as street levels compared very well with each other, the mean elevation above vegetated areas was higher in the KNC DTM and showed a higher vertical error in comparison with real time kinetic (RTK) global positioning system (GPS) measurements. The higher accuracy of the DNREC DTM in marsh areas is visible in Figure 3. For example, small tidal channels can be clearly distinguished, while channels to the north in the KNC DTM were barely detectable. This might be because flights for the KNC LiDAR were not timed with low water, and would have then measured the water surface above flooded mudflats and tidal flats.

ELEVATION ADJUSTMENTS

The existing KNC and DNREC DTMs for the model areas included vertical errors especially in densely vegetated areas which are characteristic of tidal flats. Bathymetry data were also not provided in either DTM. For both cases the DTMs had to be adjusted, as described below.

Bathymetry

Very few bathymetry measurements of tidal channels in the study marshes were available. A comprehensive measurement campaign covering all channels was not feasible at the time; hence an approach was chosen to determine the general cross-sectional shape and longitudinal slope of tidal channels based on measurements of cross-sections and on the centerline of the tidal channels. For the Blackbird Creek area water depths along 25 cross-sections (15 in the main and 10 in side channels) were measured with handheld sonar and converted to height above North American Vertical Datum of 1988 (NAVD88) based on comparison of the local water level at the time of survey to water level gauges within the area. Additionally, 60 point measurements were taken along the centerline to determine the longitudinal slope. The results showed that the shape of the main

channel is mainly trapezoidal, with the typical erosion and deposition pattern in sharp bends due to secondary flows. The longitudinal slope from the mouth to the upper reach was very small, as expected for tidal channels. In side channels, the channel depth stayed almost constant. Only near the upstream end of side channels was a distinct decrease in depth noticeable.

Initial morphodynamic numerical model tests with the model system Marina2D for the Blackbird Creek area revealed the importance of more realistic initial conditions for the bathymetry in bends. Due to a lack of data, bends in the initial model set up were often not represented correctly which led to excessive redistribution of sediments in these areas. A certain amount of bottom adjustment in the model is expected, but the time until stable conditions are reached can be decreased by improving the initial conditions.

With this in mind the sampling program for the Bombay Hook system was improved and respective locations of cross-sectional measurements were better distributed. For several bends cross-sections were taken at the beginning, center and end. From this a general shape transition for bends could be developed. A total of 48 channel cross-sections and five mudflat transects were taken (Figure 4). Mudflats occurred adjacent to the deep flow channel, in dead arms, and ponds. The water depth above a thick layer of mud was almost constantly around 0.5 m during high tide. At low tide these areas fall dry. Close to the banks a steep step up to tidal flats was visible.

Submerged channels and shallow side arms proved to be difficult to measure. Surveys were taken during high tide to ensure enough draft to enter the mudflats. This left a relatively short time window for covering considerable distances in the marsh. Additionally, the mudflat channels were covered by water at high tide and not visible anymore. Finding the deep channels and reaching them without running aground was challenging and prevented a full survey of all channels. An estimate based on measurements in similar areas was made for all channels that were not covered by the survey.

Overall the measurements suggested that the shapes of tidal channels can be generalized. The longitudinal change in depth is small enough to allow for a linear interpolation between the measured cross-sections on the existing forcing

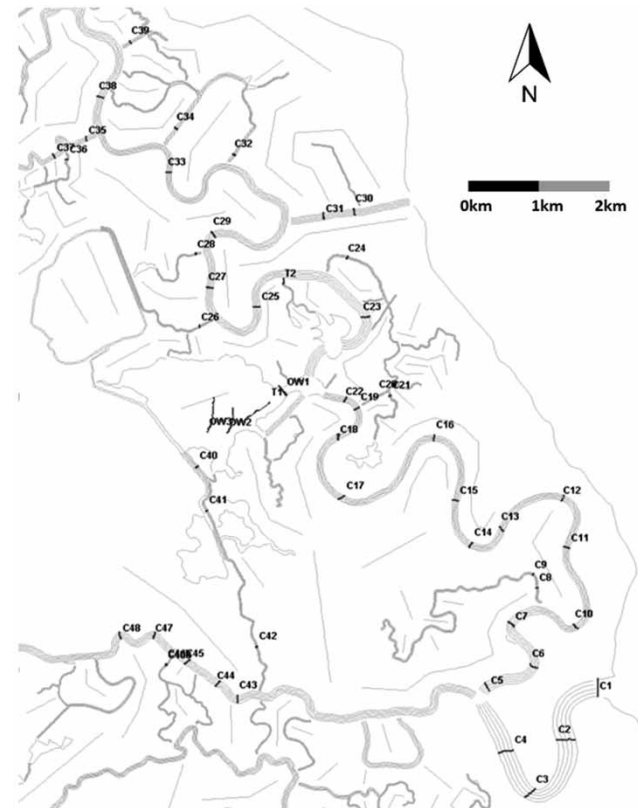


Figure 4 | Bathymetry field measurements in Bombay Hook National Wildlife Refuge.

polygons. Initial values for the interpolation were defined at measured locations and at the beginning, center and end of bends to account for the secondary profile. Final adjustments and refinements of areas with unrealistic depths were made manually.

In the time since our survey work, single beam sonar systems that are easily connected to any type of boat have become more readily available and are preferable for future surveys. They can provide high resolution bathymetry data sets with relatively little effort by surveying across channel transects in small intervals.

Ground elevation

Depending on the applied filtering method, DTMs can contain high vertical errors above areas with low and dense vegetation (Athearn *et al.* 2010; Meng *et al.* 2010; Hladik & Alber 2012; Rose *et al.* 2013). Most filtering methods search

either for the lowest elevation in a neighborhood, changes in ground surface steepness, or abrupt changes in ground heights or homogeneity (Meng *et al.* 2010). These algorithms prove not to be very useful for dense vegetation. True ground hits are rare and lowest elevation points likely represent reflections from the canopy. Marshes are low-slope environments in principle and vegetation height is often very uniform, thus easily misclassified as ground elevation (Rose *et al.* 2013). Moreover, when using readily available DTMs from public sources, the exact method used might not be specified.

The KNC DTM was created in 2007, when filtering methods for dense vegetation were rare. A high vertical error above dense vegetation was accepted as a limitation that needed to be considered for application. The DNREC DTM was specifically created for use in wetland research, thus methods were applied to ensure the best possible bare ground representation. RTK GPS elevation measurements of the ground elevation of tidal flats in the study areas were used to assess the vertical accuracy of the DTMs. A total of 660 RTK points were available for the Blackbird Creek marshes, covering most tidal flats. Their ground elevation ranged from -0.6 m NAVD88 for low-lying points to maximum elevations of $+1.1$ m close to the bay, and $+0.5$ m in the upper marsh.

The data were used to determine an upper threshold for each tidal flat. Comparison with the KNC DTM showed that the majority of its data points on tidal flats lay above their respective upper threshold, supporting the assumption that the applied filtering method overestimated the ground elevation. Elimination of the false data points was unrealistic due to their high number. Instead a constant correction factor was determined for each tidal flat based on canopy height measurements in the field and subtracted from the overestimated points. A similar approach was used by Hladik & Alber (2012) who applied plant species-specific correction factors for digital elevation model (DEM) improvement. Closer inspection of the new DTM still revealed areas with diverging elevations. Higher elevations were especially visible along shorelines (see bright areas in Figure 5). Increased growth of plants on the banks occurred due to higher sedimentation rates that provided more nutrients close to the channel, while the lower vegetation height in the tidal flat interior was relatively constant. The

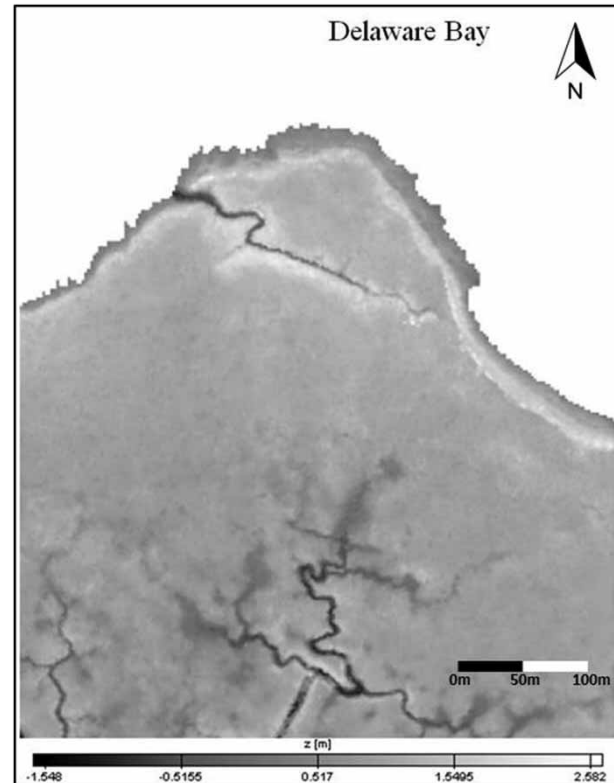


Figure 5 | Detail of KNC DTM after application of constant correction factor.

additional height was not accounted for in the correction factor and data points that were still above the aforementioned threshold were eliminated from the DTM.

To limit computational expenditure, elements on tidal flats were selected to be much coarser than those in tidal channels. This was justified because there is not much elevation change that would otherwise require the resolution of steep gradients, and there is less volume and more uniform flow across the flats. Figure 5 shows tidal channels that were too small (<9 m width) to be resolved in the model grid. However, when a mesh node coincided with a small tidal channel its low elevation was taken from the DTM resulting in steep, unrealistic elevation gradients that caused instabilities in the numerical model. To prevent this, data points within channels that were not resolved in the model mesh and were below the threshold were also eliminated from the DTM.

The accuracy of the DNREC DTM was largely sufficient, but similar adjustments in the vicinity of banks and small tidal channels were still necessary.

MESH GENERATION

Tools

For this work, a suite of software tools developed by Smile Consult GmbH (Smile 2012) was used. While GISMO was used for generating, editing, and analyzing DTMs, the numerical mesh was created using JANET, which is a multi-purpose application to produce, analyze, and optimize model meshes for a variety of numerical methods. It supports the generation of unstructured triangular meshes for finite-element methods, structured grids for finite-difference methods, and unstructured orthogonal grids for finite-volume methods. The sediment transport module of the model system Marina2D was used for the numerical simulation in the marshes.

Extraction of tidal channels

In Figures 2 and 3, the topography is depicted in flooded contours. A contour line surrounding the zone between -0.5 and $+0.5$ m NAVD88 elevation proved to produce tidal channel outlines that compared very well to existing coast lines from federal sources. These contour lines were exported as polygons and used for the subsequent extraction of significantly large tidal channels. When generating a model mesh, it is important to keep the balance between

accuracy and model efficiency. The smaller and more numerous the elements, the greater the computational effort to run the model. In this case, channels that can be resolved by at least three elements with an edge length of greater than 3 m, hence channels greater than 9 m width, were chosen to be extracted. The procedure is depicted in the schematic of Figure 6.

Both marsh systems also included wide mudflat areas whose deep, submerged channels were generally not visible in LiDAR data. Examination of aerial pictures from different years in Google Earth revealed snapshots where the deeper channels were distinctly visible with a different colour than adjacent shallow water areas. Outlines of these channels were extracted manually from Google Earth (Figure 7).

Mesh triangulation

In order to improve numerical accuracy, it is advisable to align mesh elements in areas with strong currents along the primary flow direction. In the mesh generation procedure, this was achieved by introducing 'break lines' or forcing polygons that enforced alignment of element vertices with these polygons. Figure 8 illustrates the steps taken to create the model mesh.

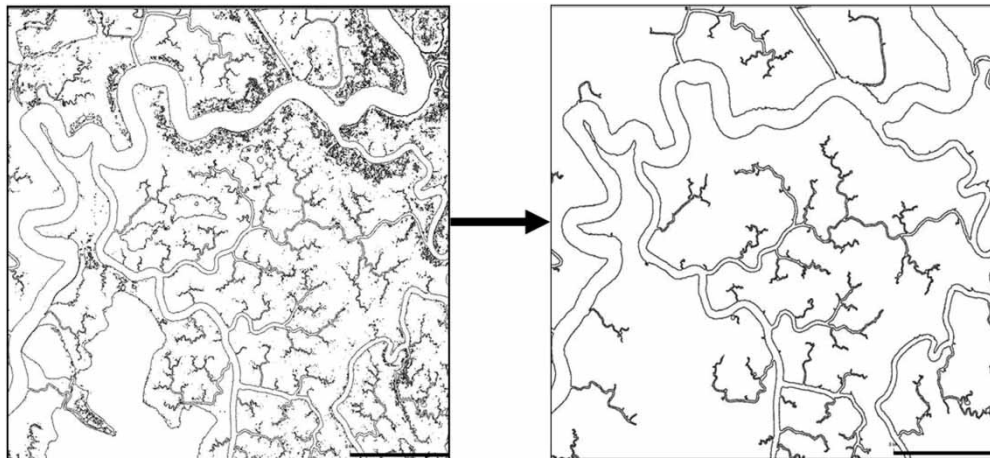


Figure 6 | Extraction of main tidal channels.

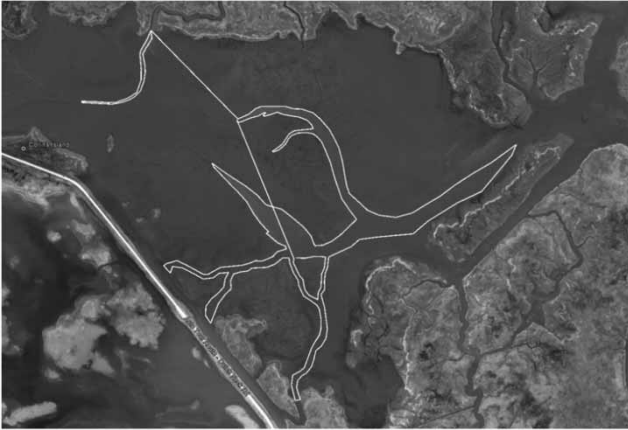


Figure 7 | Extraction of deep channels from Google Earth.

RESULTS

The mesh of the Blackbird Creek marsh system contained about 150,000 elements with maximum edge lengths of 865 m in the Delaware River and minimum lengths of 3.6 m in tidal channels (Figure 9). The area of the Bombay Hook marsh system is approximately three times as big. The number of elements was about 700,000 with a minimum edge length of 3 m in tidal channels and a maximum length of 1,000 m in the Delaware Bay (Figure 10). The connection to the Delaware River and Bay was chosen so that the boundaries are sufficiently far away from the mouths of the marsh systems but also coincide with mesh elements of a larger estuarine model that provided the forcing data for the marsh sub-models.

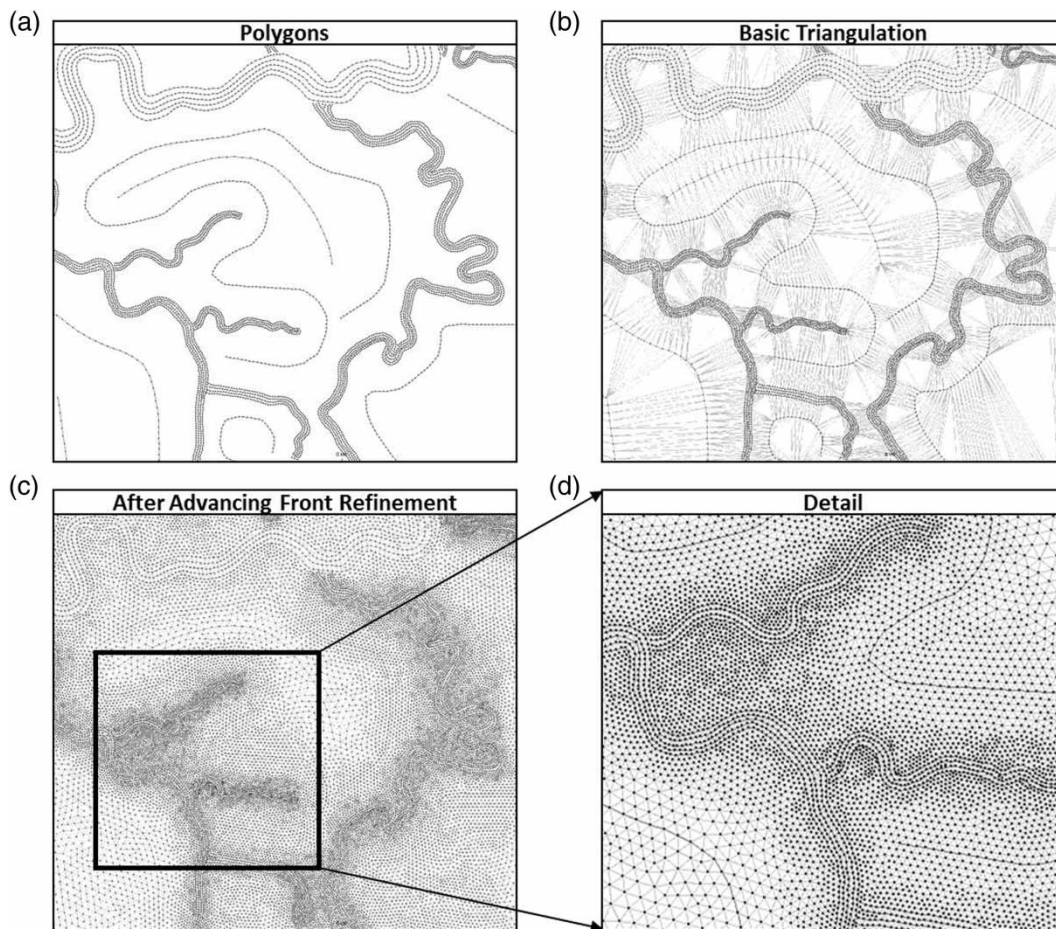


Figure 8 | Mesh triangulation steps: (a) defining the desired node distance for specific areas on forcing polygons; (b) initial triangulation; (c) and (d) advancing front step that iteratively refined the mesh while protecting nodes on the forcing polygons.

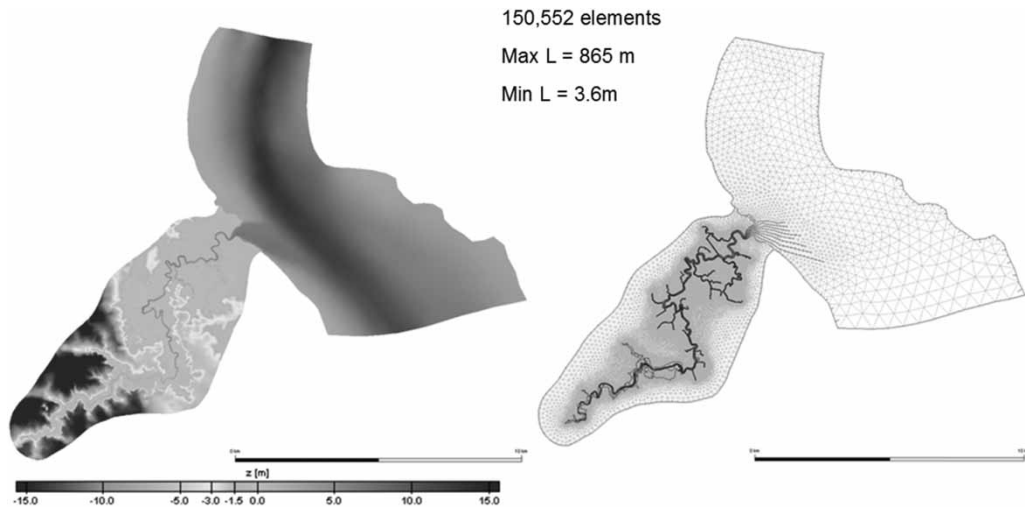


Figure 9 | Final model mesh Blackbird Creek Reserve (left: bathymetry/topography; right: mesh with forcing polygons).

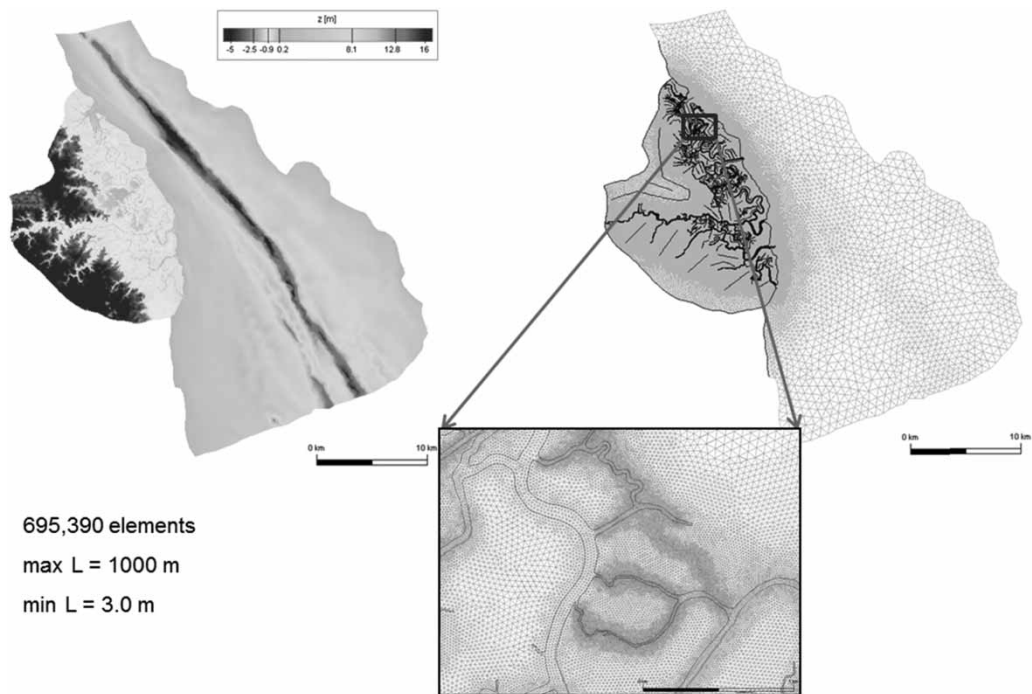


Figure 10 | Final model mesh Bombay Hook National Wildlife Refuge (left: bathymetry/topography; right: mesh with forcing polygons).

CONCLUSIONS

Users who are new to LiDAR data often find it difficult to choose from the many ground filtering algorithms. Hence, publicly available DTMs that were processed and quality controlled by LiDAR specialists are a good alternative.

However, separating ground from non-ground data still poses a significant challenge for densely vegetated areas. LiDAR-derived DTMs often overestimate the ground elevation of densely vegetated areas, especially when not created specifically for use in wetland research. It is important to assess the accuracy of existing DTMs before

application for hydrodynamic models, because inaccurate elevations can affect the numerical model output. A limited number of *in situ* ground elevation and canopy height measurements were sufficient to determine correction factors and thresholds to improve the DTMs considerably.

LiDAR data were suitable for the extraction of tidal channels and other structures that needed to be represented accurately in the model mesh. Outlines of submerged channels in open mudflats could not be detected by LiDAR and needed to be digitized manually from aerial pictures. The outlines were used as forcing polygons in the mesh generation, to ensure a balance between spatial accuracy and model efficiency.

The turbidity of water and shallow depths in wetland areas prevented bathymetrical measurements with LiDAR. Automated single beam sonar systems attached to or towed by a boat can effectively provide a high resolution bathymetrical data set. In absence of an automated system, cross-sectional bathymetrical measurements with hand held sonar and GPS positioning provided sufficient information to interpolate the bathymetry along tidal channels. Cross-section locations needed to be selected carefully to identify changes in the cross-sectional shape of channels in tight bends. Bathymetry estimates were still needed for mudflats and side channels too shallow for the boat to enter.

ACKNOWLEDGEMENTS

Funding for this work was provided by the National Oceanic and Atmospheric Administration (NOAA), Grants No. NA11NOS4200066, and the Philadelphia Water Department, Office of Watersheds (Research Assistantship). This research was also supported, in part, by a grant of computer time from the City University of New York High Performance Computing Center under NSF Grants CNS-0855217, CNS-0958379 and ACI-1126113.

REFERENCES

- Abdullah, A., Vojinovic, Z., Price, R. & Aziz, N. 2011 **A methodology for processing raw LiDAR data to support urban flood modelling framework**. *Journal of Hydroinformatics* **14** (1), 75–92.
- Abdullah, A., Vojinovic, Z., Price, R. & Aziz, N. 2012 **Improved methodology for processing raw LiDAR data to support urban flood modelling—accounting for elevated roads and bridges**. *Journal of Hydroinformatics* **14**, 253–269.
- Allen, J. R. L. 2000 **Morphodynamics of Holocene Salt marshes: A review sketch from the Atlantic and Southern North Sea coasts of Europe**. *Quaternary Science Reviews* **19**, 1155–1231.
- Athearn, N. D., Takekawa, J. Y., Jaffe, B., Hattenbach, B. J. & Foxgrover, A. C. 2010 **Mapping elevations of tidal wetland restoration sites in San Francisco Bay: Comparing accuracy of aerial Lidar with a singlebeam echosounder**. *Journal of Coastal Research* **26**, 312–319.
- Bates, P. D. 2012 **Integrating remote sensing data with flood inundation models: how far have we got?** *Hydrological Processes* **26**, 2515–2521.
- Boorman, L. A. 1999 **Salt marshes: present functioning and future change**. *Mangroves and Salt Marshes* **3**, 227–241.
- Collin, A., Long, B. & Archambault, P. 2010 **Salt-marsh characterization, zonation assessment and mapping through a dual-wavelength LiDAR**. *Remote Sensing of Environment* **114**, 520–530.
- Dewberry 2011 **Project Report regarding LiDAR data and DEM for the Bombay Hook National Wildlife Refuge**. NOAA Coastal Services Center and Delaware Department of Natural Resources and Environmental Control, Tampa, FL.
- DNREC 2013 **Blackbird Creek Reserve** [Online]. Available from: <http://www.dnrec.delaware.gov/coastal/DNERR/Pages/BlackbirdCreekReserve.aspx> [Accessed 2013].
- Gilvear, D., Tyler, A. & Davids, C. 2004 **Detection of estuarine and tidal river hydromorphology using hyper-spectral and LiDAR data: Forth estuary, Scotland**. *Estuarine, Coastal and Shelf Science* **61**, 379–392.
- Hladik, C. & Alber, M. 2012 **Accuracy assessment and correction of a LIDAR-derived salt marsh digital elevation model**. *Remote Sensing of Environment* **121**, 224–235.
- Horritt, M. S., Mason, D. C., Cobby, D. M., Davenport, I. J. & Bates, P. D. 2003 **Waterline mapping in flooded vegetation from airborne SAR imagery**. *Remote Sensing of Environment* **85**, 271–281.
- Huang, Y., Zhou, Y.-X., Li, X., Kuang, R.-Y. & Zheng, Z.-S. 2009 **Two strategies for remote sensing classification accuracy improvement of salt marsh vegetation: A case study in Chongming Dongtan**. In: 2nd International Congress on Image and Signal Processing, CISP '09, 17–19 October 2009. IEEE Computer Society, Tianjin University of Technology, Tianjin, China.
- Kathilankal, J. C., Mozdzer, T. J., Fuentes, J. D., D'odorico, P., Mcglathery, K. J. & Zieman, J. C. 2008 **Tidal influences on carbon assimilation by a salt marsh**. *Environmental Research Letters* **3**, 044010.
- Kearney, M. S. & Stevenson, J. C. 1991 **Island land loss and marsh vertical accretion rate: evidence for historical sea-level changes in Chesapeake Bay**. *Journal of Coastal Research* **7**, 403–415.

- Mason, D. C., Scott, T. R. & Hai-Jing, W. 2006 Extraction of tidal channel networks from airborne scanning laser altimetry. *ISPRS Journal of Photogrammetry and Remote Sensing* **61**, 67–83.
- Mendelssohn, I. A. & Kuhn, N. L. 2003 Sediment subsidy: Effects on soil-plant responses in a rapidly submerging coastal salt marsh. *Ecological Engineering* **21**, 115–128.
- Meng, X., Currit, N. & Zhao, K. 2010 Ground filtering algorithms for airborne LiDAR data: a review of critical issues. *Remote Sensing* **2**, 833–860.
- Milbradt, P. 2012 *Simulationsmodell Marina. Manual*. Smile Consult GmbH, Hannover, Germany.
- NOAA 2007 2007 Delaware Coastal Programs Lidar: Kent and New Castle Counties [Online]. Available from: http://csc.noaa.gov/dataviewer/webfiles/metadata/de2007_kent_newcastle_template.html [Accessed 2010].
- NOAA. 2012 Digital Coast: NOAA Coastal Services Center [Online]. Available from: <http://www.csc.noaa.gov/dataviewer/#> [Accessed 2010].
- Rose, L. S., Seong, J. C., Ogle, J., Beute, E., Indridason, J., Hall, J. D., Nelson, S., Jones, T. & Humphrey, J. 2013 Challenges and lessons from a wetland LiDAR project: a case study of the Okefenokee Swamp, Georgia, USA. *Geocarto International* **28**, 210–226.
- Rosso, P. H., Ustin, S. L. & Hastings, A. 2006 Use of lidar to study changes associated with *Spartina* invasion in San Francisco Bay marshes. *Remote Sensing of Environment* **100**, 295–306.
- Sampson, C. C., Fewtrell, T. J., Duncan, A., Shaad, K., Horritt, M. S. & Bates, P. D. 2012 Use of terrestrial laser scanning data to drive decimetric resolution urban inundation models. *Advances in Water Resources* **41**, 1–17.
- Smile 2012 Smile Consult GmbH [Online]. Available from: <http://www.smileconsult.de> [Accessed 2010].
- Valencik, K. 2010 Seal Level Rise: Delaware's Rising Tide. *Outdoor Delaware Magazine*. Delaware Department of National Resources and Environmental Control, Dover, DE.
- Wang, C.-K. & Philpot, W. D. 2007 Using airborne bathymetric lidar to detect bottom type variation in shallow waters. *Remote Sensing of Environment* **106**, 123–135.
- Wang, C., Menenti, M., Stoll, M. P., Feola, A., Belluco, E. & Marani, M. 2009 Separation of ground and low vegetation signatures in LiDAR measurements of salt-marsh environments. *IEEE Transactions on Geoscience and Remote Sensing* **47**, 2014–2023.

First received 19 March 2013; accepted in revised form 27 November 2013. Available online 28 January 2014